

# ISO observations of a sample of 60 $\mu\text{m}$ peaker galaxies

R.J. Laureijs<sup>1</sup>, D. Watson<sup>2</sup>, L. Metcalfe<sup>1</sup>, B. McBreen<sup>2</sup>, B. O'Halloran<sup>2</sup>, J. Clavel<sup>1</sup>, K. Leech<sup>1</sup>, P. Gallais<sup>1</sup>, P. Barr<sup>1</sup>, M. Delaney<sup>3</sup>, L. Hanlon<sup>2</sup>, and F. Quilligan<sup>2</sup>

<sup>1</sup> ISO Data Centre, Astrophysics Division, Space Science Department of ESA, Villafranca del Castillo, P.O. Box 50727, 28080 Madrid, Spain

<sup>2</sup> Department of Physics, University College, Dublin 4, Ireland

<sup>3</sup> Stockholm Observatory, 133 36 Saltsjöbaden, Sweden

Received 2 December 1999 / Accepted 22 April 2000

**Abstract.** The sample of IRAS galaxies with spectral energy distributions that peak near 60  $\mu\text{m}$  are called Sixty Micron Peakers (SMPs or 60PKs). Their generally peculiar and amorphous morphologies, hot dust and lack of a cirrus component have been interpreted as being indicative of a recent interaction/merger event. Mid-infrared spectra of eight SMPs, obtained with ISOPHOT-S in the  $\sim 2\text{--}11 \mu\text{m}$  band are presented. Four of the observed sources are H II region-like (H2) galaxies, three are Seyfert 2 and one is unclassified. Emission attributed to Polycyclic Aromatic Hydrocarbons (PAHs) at 6.2  $\mu\text{m}$ , 7.7  $\mu\text{m}$  and 8.6  $\mu\text{m}$  is ubiquitous in the spectra. The PHOT-S spectrum of the H2 galaxy IRAS 23446+1519 exhibits a bright 11.04  $\mu\text{m}$  line and an 8.6  $\mu\text{m}$  feature of comparable size to its 7.7  $\mu\text{m}$  feature. [S IV] emission at 10.5  $\mu\text{m}$  was detected in three of four H2 galaxies and in one Seyfert 2 galaxy. The ratio of the 7.7  $\mu\text{m}$  PAH feature to the continuum at 7.7  $\mu\text{m}$  (PAH L/C) divides the eight SMPs at a ratio greater than 0.8 for H2 and less than 0.8 for Seyfert galaxies. An anti-correlation between PAH L/C and the ratio of the continuum flux at 5.9  $\mu\text{m}$  to the flux at 60  $\mu\text{m}$  is found, similar to that found in ultraluminous infrared galaxies. Silicate absorption at approximately 9.7  $\mu\text{m}$  was observed in the Seyfert 2 galaxy, IRAS 04385-0828 and in IRAS 03344-2103. The previously unclassified SMP galaxy IRAS 03344-2103 is probably a Seyfert 2.

**Key words:** ISM: dust, extinction – ISM: molecules – galaxies: ISM – galaxies: Seyfert – galaxies: starburst – infrared: galaxies

## 1. Introduction

IRAS galaxies with spectral energy distributions peaking near 60  $\mu\text{m}$  (Vader et al., 1993) are known as Sixty Micron Peakers (SMPs or 60PKs). Vader et al. (1993) constructed the sample using the IRAS flux ratios  $f_{60}/f_{100} > 1$  and  $1 < f_{60}/f_{25} < 4$  to select extragalactic sources with galactic latitude  $|b| > 10^\circ$  from the second version of the IRAS Point Source Catalogue. There are only 51 galaxies in the sample, constituting about 2% of the space density of 60  $\mu\text{m}$ -selected galaxies in the range

$L_{60 \mu\text{m}} = 10^9\text{--}10^{12}L_\odot$  that have been identified out to a redshift of 0.2.

All SMPs are strong emission-line galaxies (Vader et al., 1993). The optical line ratio criteria of Veilleux & Osterbrock (1987) have been used to classify SMPs as H II region-like (H2) or Seyfert (Sy) galaxies. Of the 41 SMPs that have been classified, 23 are Sy2, 5 are Sy1 and 13 are H2. Approximately 60% of SMPs are therefore Seyfert galaxies. This fraction is far higher than the percentage of Seyferts found in samples of ultraluminous IRAS galaxies (Heisler & Vader, 1994). There are very few Sy1 galaxies in the full sample and none of the galaxies presented here is a Sy1. Only 4 of a sample of 45 SMPs have spiral optical morphologies, the majority being amorphous and peculiar (Heisler & Vader, 1994). The paucity of spiral galaxies is another notable feature of SMPs, since IRAS galaxies are typically spirals. The luminosity range of SMPs of about three orders of magnitude, spans the classes from dwarf galaxies to giant ellipticals.

Near-infrared (NIR) brightness profiles of H2 galaxies are well modelled by a single  $r^{1/4}$  fit but an additional nuclear point source component is required to fit the majority of Seyfert galaxy profiles (Heisler & Vader, 1995). The radio continuum and H $\alpha$  emission is compact, indicating that the FIR radiation is also emitted from a small volume (Heisler et al., 1998). The compact region has an extent of a few kpc which is comparable in size to typical narrow emission-line regions in AGN. The central region of SMPs therefore appears to be dominated by strong non-thermal or starburst emission. This emission is heavily obscured at optical wavelengths. A short-lived phase of central activity, caused by a recent interaction/merger, accounts for the morphology, the brightness near 60  $\mu\text{m}$  and the strong non-thermal or starburst source (Heisler & Vader, 1995).

The  $f_{60}/f_{100} > 1$  criterion preferentially selects galaxies with warmer or more centrally located dust. The ‘cirrus’ component which is the dominant contributor to the 100  $\mu\text{m}$  flux in spiral galaxies must therefore be weak or absent in SMPs (Vader et al., 1993). Very small grains (VSGs) of carbonaceous material contribute strongly to the flux between 25 and 60  $\mu\text{m}$  (Désert et al., 1990; Laureijs, 1998) and SMPs may be dominated by emission from VSGs. There is still

Send offprint requests to: D. Watson (dwatson@bermuda.ucd.ie)

**Table 1.** Observations of SMPs

| IRAS<br>Galaxy | R.A.  |    |       | z   | Archive<br>TDT No. | Date |        |          |            |
|----------------|-------|----|-------|-----|--------------------|------|--------|----------|------------|
|                | J2000 |    |       |     |                    |      |        |          |            |
|                | h     | m  | s     | °   | '                  | "    |        |          |            |
| 00160-0719     | 00    | 18 | 35.90 | -07 | 02                 | 57.5 | 0.0180 | 74900248 | 03/12/1997 |
| 01475-0740     | 01    | 50 | 02.50 | -07 | 25                 | 49.3 | 0.0177 | 76300953 | 17/12/1997 |
| 02530+0211     | 02    | 55 | 34.99 | +02 | 23                 | 12.9 | 0.0276 | 82101050 | 13/02/1998 |
| 03344-2103     | 03    | 36 | 39.00 | -20 | 54                 | 06.4 | 0.0058 | 81201754 | 05/02/1998 |
| 04385-0828     | 04    | 40 | 55.48 | -08 | 23                 | 06.6 | 0.0151 | 83301373 | 25/02/1998 |
| 05189-2524     | 05    | 21 | 01.40 | -25 | 21                 | 45.9 | 0.0419 | 70102085 | 17/10/1997 |
| 08007-6600     | 08    | 01 | 09.39 | -66 | 08                 | 33.1 | 0.0412 | 72401151 | 09/11/1997 |
| 23446+1519     | 23    | 47 | 08.64 | +15 | 36                 | 16.1 | 0.0258 | 56500952 | 03/06/1997 |

some debate as to the actual carriers of the CH and CC aromatic bonds that produce emission features that dominate in the 3–13  $\mu\text{m}$  spectral region of spiral galaxies (Lu et al., 1999) and Seyferts (Clavel et al., 1999). It is commonly assumed that the emission is produced by polycyclic aromatic hydrocarbons (PAHs) but other models exist such as the ‘Coal Model’ (Papoular et al., 1989; Guillois et al., 1998). Laboratory and theoretical results based on PAH mixtures fit the observed spectra consistently (Salama, 1998; Boulanger et al., 1998; Moutou et al., 1998; Langhoff, 1996). The features at 3.3, 6.2, 7.7, 8.6 and 11.3  $\mu\text{m}$  are therefore referred to as ‘PAH emission’ hereafter. PAH emission is complex (Peeters et al., 1999; Boulanger et al., 1998; Langhoff, 1996) and varies spatially within galaxies (Tielens et al., 1999; Moorwood, 1999). The 2–11  $\mu\text{m}$  spectra of SMPs are expected to be largely dominated by the ubiquitous PAH emission. Their spectra should however be modified by direct emission from non-thermal or starburst components and from hot dust (VSGs) (Désert et al., 1990). The presence of high energy photons will also modify the spectrum indirectly by exciting and destroying different PAHs preferentially depending on their composition (Uchida et al., 1998; Roelfsema et al., 1996).

Sect. 2 details observations of eight SMPs with the ISOPHOT photopolarimeter (Lemke et al., 1996) on board the Infrared Space Observatory (ISO) (Kessler et al., 1996). Results of the observations and a discussion are presented in Sect. 3. The separation of H2 and Sy galaxies is discussed in Sect. 4. Conclusions are in Sect. 5. In this paper,  $H_0 = 75 \text{ km s}^{-1} \text{ Mpc}^{-1}$  and  $q_0 = 0.5$  are adopted.

## 2. Observations and data reduction

Eight of the brightest SMPs visible to ISO were selected for observation with ISOPHOT-S being roughly representative of the full SMP sample. Four of the galaxies are H2, three are Sy2, and the classification of one is uncertain. Observations were carried out between December 1997 and February 1998. Table 1 lists the R.A., Dec. and the redshift of the galaxies as well as the ISO data archive number and the date of the observation.

PHT-S consists of a dual grating spectrometer with a resolving power of  $\lambda/\Delta\lambda \sim 90$  in two wavelength bands. Band SS covers the wavelength range 2.5–4.8  $\mu\text{m}$ , while band SL covers

the range 5.8–11.8  $\mu\text{m}$  (Laureijs et al., 1998). PHT-S measurements were made in chopped mode, using either rectangular or triangular chopping with the ISOPHOT focal-plane chopper; the mode depending on the difficulties of avoiding any nearby sources. During the chop cycle, 512 seconds were spent on-target and 512 seconds off-target – either in a single off-target pointing, or two 256 second off-target pointings. Chopper throw ranged from about 1–3' depending on the extent of the target source and the density of surrounding field sources. The calibration of the spectrum was performed using a spectral response function derived from several calibration stars of different brightnesses observed in a mode similar to that of the observation of the target (Acosta-Pulido, 1999). The relative photometric uncertainty of the PHT-S spectrum is better than 20% when comparing different parts of the spectrum that are more than a few microns apart. The absolute photometric uncertainty is better than 30% for bright calibration sources (Schulz, 1999). All data processing was performed using the ISOPHOT Interactive Analysis (PIA V7.22) system (Gabriel, 1998). Data reduction consisted primarily of the removal of instrumental effects such as cosmic ray glitches. After background subtraction was performed, flux densities for the sources were determined. In order to increase the signal-to-noise ratio per channel the spectra were smoothed using:

$$a_{s_n} = (0.25 \times a_{n-1}) + (0.5 \times a_n) + (0.25 \times a_{n+1}) \quad (1)$$

where  $a_n$  is the flux in channel n and  $a_{s_n}$  is the smoothed flux in channel n. Using this method, the flux is effectively spread over 2 channels in a way that does not change the position of the spectral peaks and which conserves the flux. These fluxes were then corrected for redshift to obtain rest-frame spectra. The PHT-S band fluxes were derived from these spectra. An estimate of the continuum was made following the method of Lutz et al. (1998). A linear interpolation between the fluxes at 5.9 and 10.9  $\mu\text{m}$  was used except for the sources IRAS 01475-0740, IRAS 08007-6600 and IRAS 23446+1519. For these source, a linear interpolation between the minimum flux values near 6  $\mu\text{m}$  and 10.5  $\mu\text{m}$  was used instead to estimate the continuum. Flux errors were determined by adding in quadrature the  $1 \sigma$  errors of all the bins in the feature. Upper limits were derived at the  $3 \sigma$  level of significance.

**Table 2.** ISOPHOT Fluxes with IRAS fluxes listed for comparison.  $f_{60}/f_{\text{PHT}}$  is the IRAS 60  $\mu\text{m}$  flux divided by the PHT-SL flux. The spectral classification of the galaxies is adopted from Vader et al. (1993)

| IRAS<br>GALAXY | ISO Fluxes (mJy) |             | IRAS Fluxes (Jy) |                  |                  |                   | FIR/MIR<br>$f_{60}/f_{\text{PHT}}$ | EW ( $\mu\text{m}$ )<br>(7.7 $\mu\text{m}$ ) | PAH L/C<br>(7.7 $\mu\text{m}$ ) | Spec.<br>Type |
|----------------|------------------|-------------|------------------|------------------|------------------|-------------------|------------------------------------|--|---------------------------------|---------------|
|                | PHT-SS           | PHT-SL      | 12 $\mu\text{m}$ | 25 $\mu\text{m}$ | 60 $\mu\text{m}$ | 100 $\mu\text{m}$ |                                    |  |                                 |               |
| 00160-0719     | 21 $\pm$ 2       | 65 $\pm$ 2  | <0.26            | 0.63             | 1.79             | 1.54              | 39                                 | 4.7  | 1.9                             | H2            |
| 01475-0740     | 16 $\pm$ 2       | 119 $\pm$ 2 | 0.28             | 0.83             | 1.1              | <1.05             | 12                                 | 0.6  | 0.2                             | Sy2           |
| 02530+0211     | 11 $\pm$ 2       | 58 $\pm$ 2  | <0.25            | 0.81             | 2.77             | 1.79              | 45                                 | 2.6  | 1.6                             | H2            |
| 03344-2103     | 50 $\pm$ 6       | 276 $\pm$ 6 | 0.41             | 1.91             | 7.23             | 5.96              | 22                                 | (0.8)†                                       | 0.8                             | ?             |
| 04385-0828     | 84 $\pm$ 3       | 289 $\pm$ 2 | 0.45             | 1.67             | 2.95             | 2.14              | 11                                 | 0.1  | 0.3                             | Sy2           |
| 05189-2524     | 131 $\pm$ 4      | 359 $\pm$ 2 | 0.76             | 3.52             | 13.94            | 11.68             | 45                                 | 0.3  | 0.4                             | Sy2           |
| 08007-6600     | 40 $\pm$ 1       | 177 $\pm$ 2 | 0.27             | 1.11             | 3.7              | 3.19              | 24                                 | 0.5  | 0.9                             | H2            |
| 23446+1519     | 17 $\pm$ 2       | 56 $\pm$ 3  | <0.25            | 1.22             | 4.2              | 3.54              | 100                                | 8.0  | 4.4                             | H2            |

† Tentative

**Table 3.** Emission line fluxes or upper limits ( $10^{-15} \text{ W m}^{-2}$ ) and estimates of the continuum(C) at the centre of the line ( $10^{-15} \text{ W m}^{-2} \mu\text{m}^{-1}$ ) for the eight sources observed with ISOPHOT.

| Lines<br>$\lambda$ ( $\mu\text{m}$ ) | PAH<br>6.2    | C    | PAH<br>6.67    | C    | PAH<br>7.7  | Luminosity<br>$\times 10^{34} \text{ W}$ | C    | PAH<br>8.6     | C    | [S IV]<br>10.5 | C    |
|--------------------------------------|---------------|------|----------------|------|-------------|--|------|----------------|------|----------------|------|
| 00160-0719                           | 2.2 $\pm$ 0.4 | 1.2  | <0.9           | 1.3  | 18 $\pm$ 2  | 11                                       | 1.4  | 4.6 $\pm$ 1.2  | 1.5  | 1.0 $\pm$ 0.4  | 1.5  |
| 01475-0740                           | <0.9          | 3.0  | 0.9 $\pm$ 0.2  | 3.2  | 15 $\pm$ 2  | 9  | 3.4  | <6.5           | 3.5  | 0.7 $\pm$ 0.2  | 3.4  |
| 02530+0211                           | <1.9          | 3.0  | 0.9 $\pm$ 0.03 | 2.7  | 59 $\pm$ 2  | 86                                       | 2.3  | <3.5           | 2.0  | <0.6           | 1.5  |
| 03344-2103                           | <10.8         | 22.5 | <13.7          | 18.8 | 299 $\pm$ 5 | 19                                       | 12.1 | <6.3           | 7.7  | <1.5           | 2.5  |
| 04385-0828                           | <3.4          | 16.6 | 1.5 $\pm$ 0.2  | 14.8 | 79 $\pm$ 2  | 35                                       | 12.4 | 15 $\pm$ 1     | 10.2 | <0.2           | 7.5  |
| 05189-2524                           | 2.8 $\pm$ 0.4 | 18.6 | <0.4           | 17.3 | 91 $\pm$ 2  | 309                                      | 15.2 | 13.9 $\pm$ 0.8 | 13.6 | <0.6           | 11.1 |
| 08007-6600                           | 5.8 $\pm$ 0.3 | 7.5  | <1.3           | 6.7  | 89 $\pm$ 2  | 296                                      | 5.6  | 18 $\pm$ 1     | 4.7  | 1.8 $\pm$ 0.4  | 3.5  |
| 23446+1519                           | 2.4 $\pm$ 0.7 | 0.6  | 0.6 $\pm$ 0.1  | 0.5  | 41 $\pm$ 2  | 55                                       | 0.5  | 9.6 $\pm$ 1.3  | 0.4  | 2.7 $\pm$ 1.0  | 0.3  |

### 3. Results and discussion

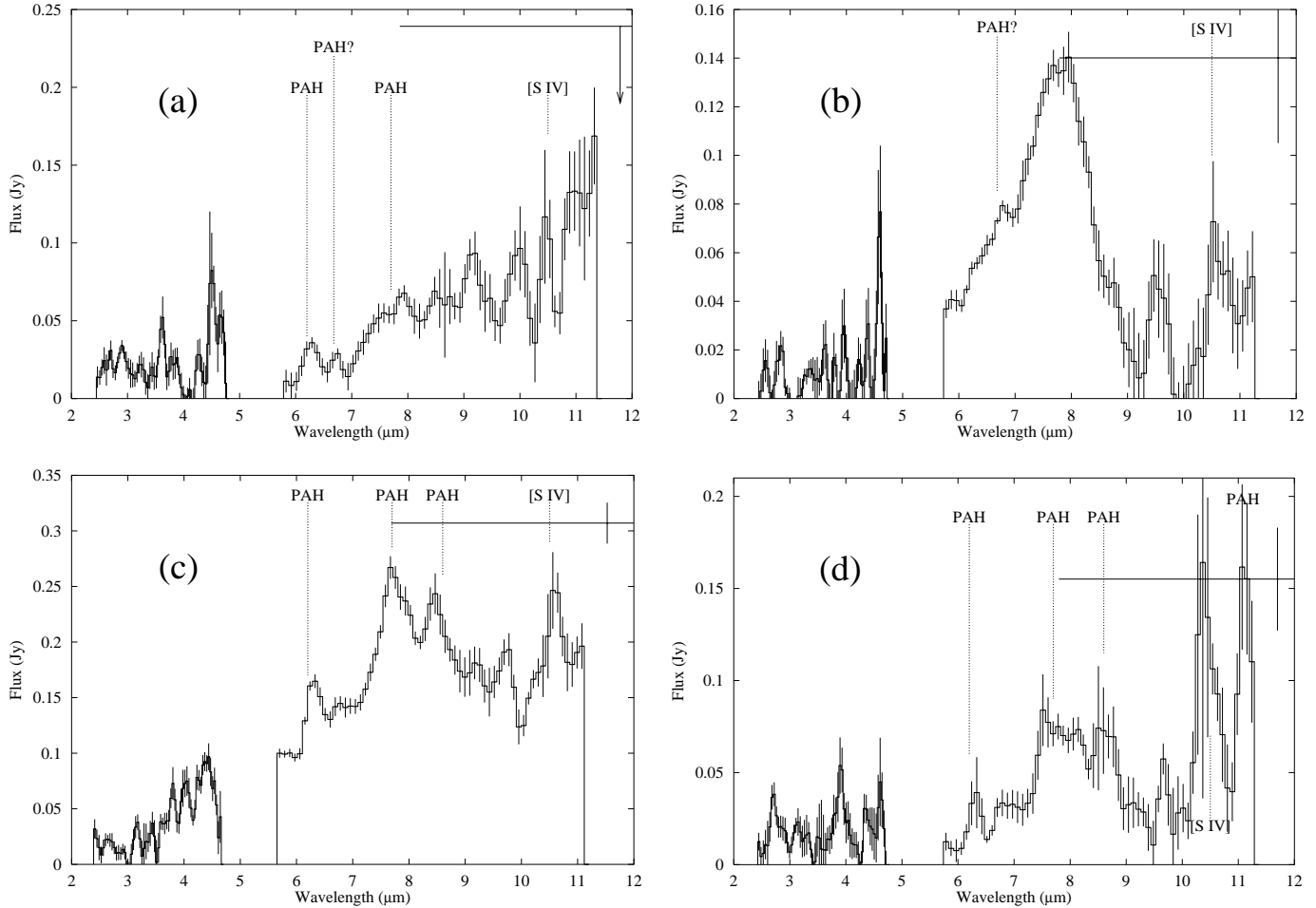
Spectra of eight SMP galaxies are presented in Figs. 1 and 2. The results of these observations are summarised in Tables 2 and 3. Table 2 lists ISOPHOT and IRAS fluxes, ratios of the IRAS 60  $\mu\text{m}$  to the PHT-SL flux, the equivalent width (EW) of the 7.7  $\mu\text{m}$  PAH feature and the PAH to continuum ratios at 7.7  $\mu\text{m}$  (PAH L/C), as well as the optical spectral classification of the galaxies. It is clear from Table 2 that the ratio of IRAS 60  $\mu\text{m}$  flux to the PHT-SL flux is generally higher in the H2 galaxies than it is in the Seyferts. The EW is more uncertain in galaxies with broad PAH features where the spectrum is heavily absorbed by silicate (e.g. Fig. 2d). The 7.7  $\mu\text{m}$  PAH EWs are generally larger in the H2 galaxies. The ratio of the height of the 7.7  $\mu\text{m}$  feature above the continuum to the continuum level at 7.7  $\mu\text{m}$  is referred to as PAH L/C (Table 2). The continuum was obtained from a linear interpolation between points near 5.9  $\mu\text{m}$  and 10.9  $\mu\text{m}$  as described in the previous section. This ratio is a measure of the relative importance of PAH in the total emission from the galaxy, and has been shown to be a good discriminator between starburst and AGN in a sample of Ultraluminous Infrared Galaxies (ULIRGs) (Lutz et al., 1998; Genzel et al., 1998). Applying this ratio to SMPs shows that it can discriminate between H2 and Seyfert galaxies (Table 2).

Table 3 lists the line fluxes, and an estimate of the continuum at the centre of the lines. The luminosities of the 7.7  $\mu\text{m}$  PAH

feature are also listed in Table 3. The 7.7  $\mu\text{m}$  luminosity gives a better estimate of the amount of PAH in the galaxy than the other PAH features between 5 and 11  $\mu\text{m}$ , which are more prone to dust-extinction (Rigopoulou et al., 1999). The luminosity of this feature appears to be independent of spectral type (Table 3 and Clavel et al. 1999).

The emission feature at  $\sim 6.7 \mu\text{m}$  (Table 3) exists in the spectra of two H2 and one Sy2 galaxy. It is labelled ‘PAH?’ in Figs. 1 and 2 and is identified with the weak PAH feature at 6.66  $\mu\text{m}$  (Peeters et al., 1999).

Emission features between 9  $\mu\text{m}$  and 11  $\mu\text{m}$  exist in the spectra of 3 H2 galaxies; IRAS 00160-0719, IRAS 02530+0211 and IRAS 23446+1519 (Figs. 1b,c and d) and in one Sy2 IRAS 01475-0740 (Fig. 2a) and may be attributable to PAH. Another possibility however, is that these narrow peaks may be emission features from crystalline silicates (Watson et al. in preparation). Crystalline silicates have already been detected in solar system comets (Hanner et al., 1994; Crovisier et al., 1997), interplanetary dust particles (Bradley et al., 1998), the disks surrounding young stars (Malfait et al., 1998; Waelkens et al., 1998) and in the outflows of evolved stars (Waters et al., 1998). Crystalline silicate can be produced in a condensation sequence such as that around oxygen-rich AGB stars or by annealing amorphous silicate at temperatures near 1000 K (Molster et al., 1999) or perhaps by a low-temperature annealing process (Molster et al., 1999). For



**Fig. 1a–d.** PHT-S spectra of the H2 galaxies: **a** IRAS 00160-0719, **b** IRAS 02530+0211, **c** IRAS 08007-6600, **d** IRAS 23446+1519. The IRAS 12  $\mu\text{m}$  flux or upper limit is plotted for comparison.

spectra with peaks near 9.1  $\mu\text{m}$ , assuming they are produced by hypersthene at 300 K, the mass of crystalline silicate required to produce this emission is  $\sim 1 M_{\odot}$  in IRAS 00160-0719 and  $\sim 1.6 M_{\odot}$  in IRAS 01475-0740. Spectral observations at longer wavelengths should also reveal features due to crystalline silicate emission, further assisting identification of these minerals. Observations of these longer wavelength features are important in studies of stellar sources (Waters et al., 1998).

Though the PHT-SL band extends to 11.8  $\mu\text{m}$ , the PAH emission at  $\sim 11.3 \mu\text{m}$  is difficult to detect in these spectra due to the redshift of the galaxies. It can be difficult to distinguish absorption at  $\sim 9.7 \mu\text{m}$  due to silicate, from an artefact caused by broad PAH emission at  $\sim 8 \mu\text{m}$  and 11.3  $\mu\text{m}$  (Roche, 1989). Silicate absorption is probably present in the spectra of IRAS 04385-0828 and IRAS 03344-2103 (Figs. 2b and 2d respectively). The shape of the trough at 9.7  $\mu\text{m}$ , the clearly rising continuum in the PHT-SS band, and the IRAS 12  $\mu\text{m}$  fluxes all provide strong evidence that the absorption features in these two spectra are not artefacts. Noise dominates PHT-SS spectra with fluxes less than  $\sim 0.05$  Jy. It is clear however that there is a strong signal in the long wavelength end of the PHT-SS spectra of IRAS 04385-0828 and IRAS 03344-2103.

### 3.1. H2 galaxies

The spectra of the four H2 galaxies (Fig. 1) are all dominated by emission features associated with PAHs between 6 and 9  $\mu\text{m}$ , though IRAS 08007-6600 (Fig. 1c) clearly has a strong MIR continuum. The PAH emission in IRAS 02530+0211 appears to be a blend of the standard 7.7 and 8.6  $\mu\text{m}$  features in one broad peak, but absorption by silicate cannot be ruled out in this galaxy. IRAS 23446+1519 has an unusual spectrum with strong line emission near 11.0  $\mu\text{m}$  (Fig. 1d). This line has been detected in HII regions (at 11.04  $\mu\text{m}$ ) and attributed to PAHs. Roelfsema et al. (1996) have interpreted the existence of this feature in conjunction with an unusually strong 8.6  $\mu\text{m}$  band (comparable to the 7.7  $\mu\text{m}$  feature) and a 7.8  $\mu\text{m}$  shoulder on the 7.7  $\mu\text{m}$  feature as being indicative of the presence of non-compact PAHs. All these characteristics are present in the spectrum of IRAS 23446+1519. In older systems with PAH emission, the less stable non-compact PAHs will generally have been destroyed, but in a non-equilibrium situation, the non-compact PAHs can exist and modify the observed spectrum. Non-compact PAHs are probably present in IRAS 23446+1519. It is interesting to note that a very similar

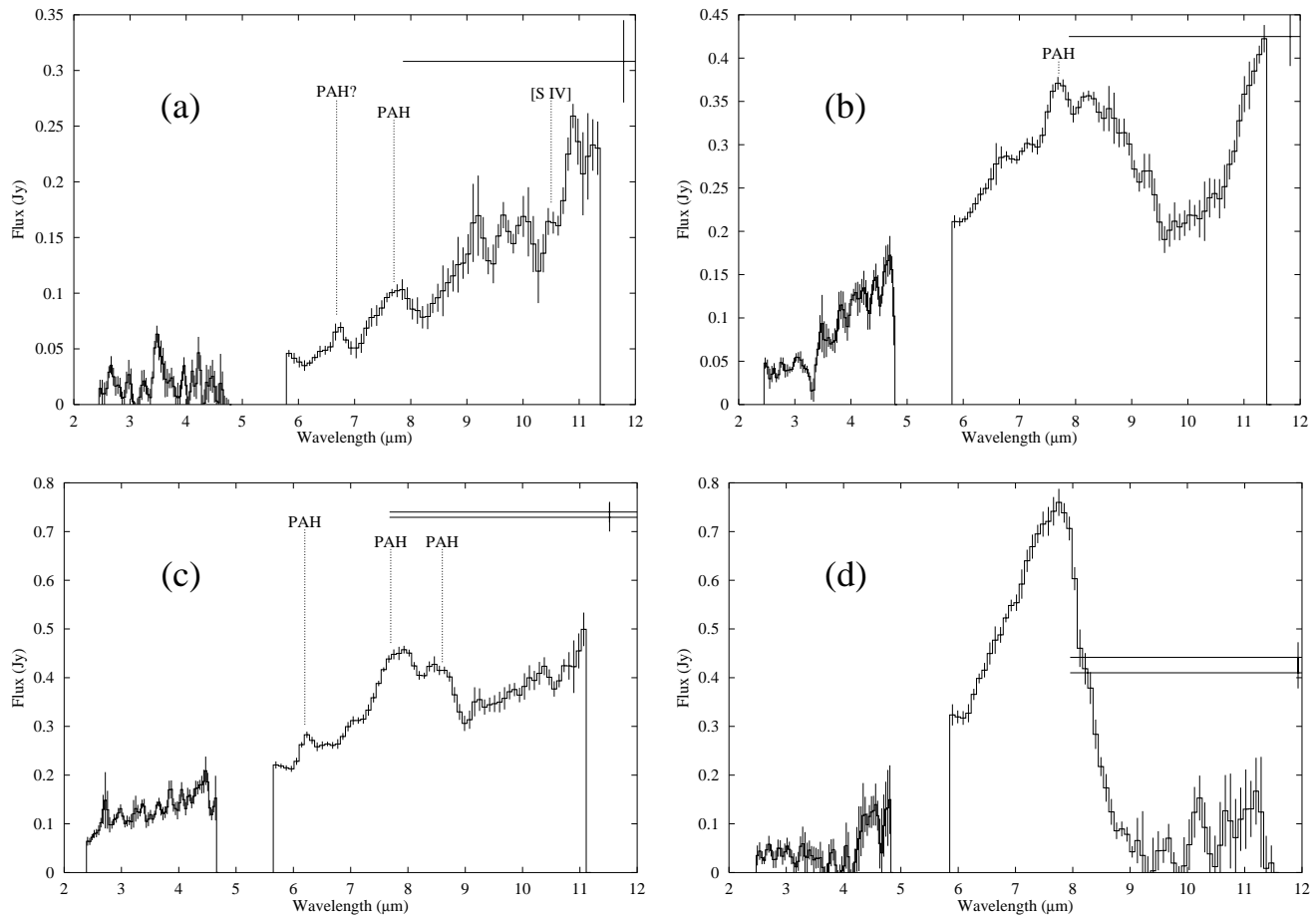


**Fig. 2a–d.** PHT-S spectra of the three Sy2 galaxies: **a** IRAS 01475-0740, **b** IRAS 04385-0828 and **c** IRAS 05189-2524, and the one unclassified galaxy: **d** IRAS 03344-2103. IRAS 12  $\mu\text{m}$  fluxes are plotted for comparison.

spectrum has been observed from the Wolf-Rayet (WR) galaxy NGC 1741 (McBreen et al. in preparation).

The broad 9.7  $\mu\text{m}$  silicate absorption feature is more common in AGN than in H2 type galaxies (Roche, 1989). Evidence of this feature is present in the spectra of two galaxies, neither of which is H2 type. [S IV] emission at 10.5  $\mu\text{m}$  was detected in three of the four H2 galaxies, but in only one Sy2 (see Table 3). Photons of a few eV are sufficient to generate standard PAH emission spectra at wavelengths shorter than 9  $\mu\text{m}$  (Uchida et al., 1998), but this is not the case with other lines emitted in the MIR. The presence of [S IV] emission implies a flux of hard photons in the region in which it is produced, assuming photo-ionisation. The more luminous MIR continuum in Seyferts would tend to diminish the signal-to-noise ratio of the [S IV] line and may explain the greater prevalence of this line in the H2 galaxies. WR stars are energetic enough to produce [S IV] emission and it should be noted that this line has already been observed in the WR galaxies Haro 3 (Metcalf et al., 1996), NGC 7714 (O’Halloran et al., 1999) and NGC 5253 (Crowther et al., 1999). Some SMPs are also classified as WR galaxies. They are NGC 5253, II Zw 40, Mrk 1210, Tol 1924-416 and possibly Tol 1345-419

(Schaerer et al., 1999). A search for the optical signature of WRs in other SMPs could reveal new WR galaxies.

### 3.2. Sy2s

In general the three Sy2 galaxies (Figs. 2a, b and c) have similar 7.7  $\mu\text{m}$  PAH luminosities (Table 3), but smaller 7.7  $\mu\text{m}$  PAH EW and L/C values than the four H2 galaxies (Table 2). It is clear from Fig. 2 that the Sy2s have significant continuum emission thus explaining their low PAH EW and L/C values. Continuum emission from a central source above that detected in H2 galaxies is necessary to explain the NIR brightness profiles of Sy2 SMPs (Heisler & Vader, 1995). This implies that some of the brighter continuum observed in these Sy2 spectra could be, directly or indirectly due to the Seyfert nucleus. The spectrum of IRAS 03344-2103 (Fig. 2d) has a very large silicate absorption trough near 9.7  $\mu\text{m}$  making it difficult to identify lines beyond  $\sim 8 \mu\text{m}$  and making the EW of 7.7  $\mu\text{m}$  feature difficult to determine.

There are clear discriminators between H2 and Sy2 galaxies in the mid-infrared. They are PAH L/C, EW and the IRAS 60  $\mu\text{m}$  to the PHT-SL flux ratio (see Table 2 and Fig. 3) and are discussed in the next section.

#### 4. Separation of starbursts and AGN

In the standard model, Sy1s and Sy2s differ in their orientation to the line of sight (Urry & Padovani, 1995). The Seyfert nucleus is surrounded by a dusty torus that obscures the broad emission-line region (BLR) in Sy2s (which are viewed edge-on).

PAH emission is produced outside the torus and is independent of the nucleus (Clavel et al., 1999). In the well-studied Sy2 Circinus galaxy, Moorwood (1999) manages explicitly to exclude the nucleus as the source of excitation for the PAH emission using ISOCAM-CVF. Clavel et al. (1999) use the EW of the 7.7  $\mu\text{m}$  feature as a discriminator between Sy1 and Sy2. Laurent et al. (1999) have proposed a similar diagnostic, using the ratio of the PAH 6.2  $\mu\text{m}$  band to the 5.1 to 6.7  $\mu\text{m}$  continuum to distinguish AGN from starburst galaxies. These are in essence a similar measure to the PAH L/C at 7.7  $\mu\text{m}$  since all depend on the facts that (a) PAH luminosities are independent of the active nucleus (Clavel et al., 1999) and (b) the MIR continuum is stronger in Sy1 than Sy2 and brighter in AGN as a whole than in starburst galaxies. Laurent et al. (1999) extend this diagnostic tool to assess the relative contributions of components from AGN, H II and photo-dissociation regions by introducing the ratio of the warm to the hot continuum. This ratio was not obtainable in the PHT-S waveband because it does not extend to 15  $\mu\text{m}$ .

In Sy1s the BLR and the inner wall of the torus are directly visible, making the MIR continuum brighter in these galaxies. In Sy2s seen fully edge-on, our line of sight to the inner wall of the torus is blocked and the MIR continuum is suppressed (Clavel et al., 1999). In the intermediate situation of Sy2 viewed at grazing incidence, one has a direct view of the inner wall of the torus but a reflected view of the BLR. This corresponds to Sy2s where the MIR continuum is strong and broad lines are observed only in polarised light (Clavel et al., 1999; Heisler et al., 1996; Heisler et al., 1997). IRAS 05189-2524 falls into this category, since it has polarised broad-lines (Young et al., 1996) and a strong MIR continuum (Fig. 2c). The 7.7  $\mu\text{m}$  PAH EW of IRAS 05189-2524 is 0.3  $\mu\text{m}$  falling in the range observed by Clavel et al. (1999) for this sub-class of Sy2. IRAS 04385-0828 has a 7.7  $\mu\text{m}$  EW of just 0.1  $\mu\text{m}$  (Table 2) and is therefore another good candidate for possessing polarised broad lines. Unfortunately, though it was observed in polarised light, the signal-to-noise ratio was not sufficiently good to determine the EW of the lines in the polarised spectrum (Young et al., 1996).

Dudley (1999) finds the 1–5  $\mu\text{m}$  SED of IRAS 05189-2524 to be similar to that of the infrared-bright quasar IRAS 13349+2438 (Beichman et al., 1986). He therefore proposes that hot dust heated by an AGN is responsible for the 1–5  $\mu\text{m}$  continuum in both sources. It is clear however that two components are required to fit the 1–100  $\mu\text{m}$  SED in IRAS 05189-2524. Dudley (1999) therefore further suggests that the 8–100  $\mu\text{m}$  emission is better explained by emission arising from star formation than from an AGN. The observation of IRAS 05189-2524 presented here shows no evidence of a spectral break between 2.5  $\mu\text{m}$  and 11  $\mu\text{m}$ . The very large IRAS 12  $\mu\text{m}$  flux for this source indicates that such a spectral

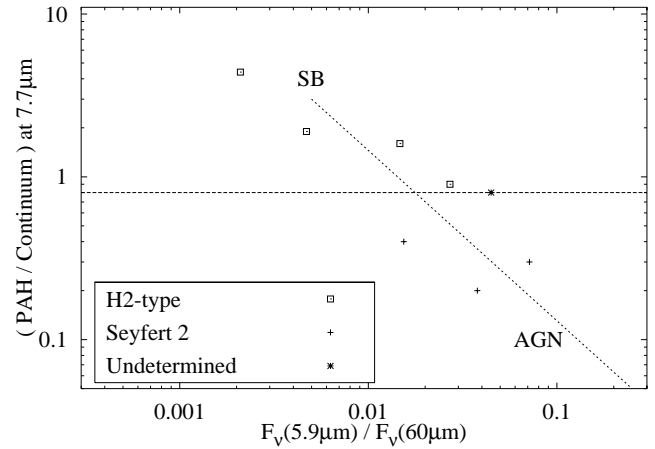


**Fig. 3.** Comparison of the ratio of 60  $\mu\text{m}$  flux to 5.9  $\mu\text{m}$  flux versus the ratio of the height of the PAH feature at 7.7  $\mu\text{m}$  to the 7.7  $\mu\text{m}$  continuum. Boxes represent H2-type galaxies, plusses are Seyfert 2 type galaxies, the asterisk is IRAS 03344-2103. The dashed line at PAH/Continuum = 0.8 divides H2 galaxies from Seyferts. “SB” and “AGN” represent unobscured starburst and AGN type emission respectively. The dotted line represents the dilution of a pure starburst spectrum by a 5.9  $\mu\text{m}$  continuum as shown by Lutz et al. (1998) for a sample of ULIRGs.

break could lie near 12  $\mu\text{m}$  (Fig. 2c). It is clear from these results that IRAS 05189-2524 is a Seyfert and that the hot inner wall of the torus is largely responsible for the 2.5  $\mu\text{m}$ –11  $\mu\text{m}$  continuum. Recent PHT-S observations of IRAS 13349+2438 (Watson et al., 1999) while showing PAH emission, also suggest that the inner wall of the torus is the source of most of the 2.5  $\mu\text{m}$ –11  $\mu\text{m}$  continuum in this quasar. The similarity in the spectra of IRAS 05189-2524 and IRAS 13349+2438 may be attributed to the suggestion that they are both AGN viewed near grazing incidence to their tori (Clavel et al., 1999; Wills et al., 1992).

The ratio of the PHT-SL 5.9  $\mu\text{m}$  flux to the IRAS 60  $\mu\text{m}$  flux is plotted against the PAH L/C values (Table 2) in Fig. 3. There is an anti-correlation between the PAH L/C and the  $F_{\nu}(5.9 \mu\text{m})/F_{\nu}(60 \mu\text{m})$  ratio indicating that warmer SMPs are more AGN-dominated, and cooler SMPs are more starburst-like. The anti-correlation is significant at a probability greater than 99% (from a Pearson’s correlation statistic of -3.7). The eight SMPs divide very well at PAH L/C = 0.8 (Fig. 3). The method Lutz et al. (1998) applied to a sample of ULIRGs is followed in Fig. 3. The same anti-correlation was found for ULIRGs as is discovered here. Lutz et al. (1998) used the criterion PAH L/C = 1 to separate AGN from starburst ULIRGs, but found this criterion tended to classify some starbursts as AGN.

IRAS 08007-6600, appears to be currently undergoing a merger and possesses two distinct nuclei (Heisler & Vader, 1994). It is possible that one of the nuclei may contain a hidden non-thermal source given its position on the Starburst-AGN plot (Fig. 3) with PAH L/C = 0.9, despite its optical classification as a H2 galaxy. The unclassified galaxy, IRAS 03344-2103 may also be a Seyfert since it shows evidence of silicate absorption in its spectrum (Fig. 2d) and has a PAH L/C = 0.8.

## 5. Conclusions

ISOPHOT-S spectra were obtained for a sample of eight SMPs of types H2 and Sy2. PAH emission was detected in all the spectra. The spectrum of IRAS 23446+1519 shows an unusual 8.6  $\mu\text{m}$  feature with a height comparable to the 7.7  $\mu\text{m}$  feature and exhibits a very bright 11.04  $\mu\text{m}$  PAH emission line. The spectrum implies that non-compact PAHs are the source of a large proportion of the PAH emission in that galaxy. [S IV] emission is more prevalent in the H2 galaxies than in the Sy2s, probably because of the brighter continuum in Sy2s. Silicate absorption ( $\sim 9.7 \mu\text{m}$ ) was observed in IRAS 03344-2103 and in IRAS 04385-0828. The results show that the H2 galaxies have PAH L/C at 7.7  $\mu\text{m}$   $> 0.8$  and the Sy2 galaxies have PAH L/C  $\leq 0.8$ . The same anti-correlation exists in SMPs and ULIRGs between the PAH L/C and the  $F_{\nu}(5.9 \mu\text{m})/F_{\nu}(60 \mu\text{m})$  ratio. It is proposed that IRAS 08007-6600 may contain a hidden non-thermal source and that the previously unclassified galaxy IRAS 03344-2103 may be a Seyfert. Observations of IRAS 04385-0828 may reveal broad emission lines in polarised light.

While the galaxies presented here are diverse, observation of a larger sample of SMPs in the mid-infrared could confirm the Seyfert/H2 separation and the anti-correlation observed here. The prevalence of [S IV] emission in H2 SMPs implies that a search of SMP optical spectra for the WR signature may reveal new WR galaxies.

## References

- Acosta-Pulido J., 1999, [http://www.iso.vilspa.esa.es/users/expl.lib/PHT/chop\\_report02.ps.gz](http://www.iso.vilspa.esa.es/users/expl.lib/PHT/chop_report02.ps.gz)
- Beichman C.A., Soifer B.T., Helou G., et al., 1986, *ApJ* 308, L1
- Boulanger F., Boissel P., Cesarsky D., Ryter C., 1998, *A&A* 339, 194
- Bradley J.P., Snow T.P., Brownlee D.E., Hanner M.S., 1998, In: d'Hendecourt L., Joblin C., Jones A. (eds.), *Solid interstellar matter: the ISO revolution*, Vol. 11, pp 297–315, Les Houches Workshop
- Clavel J., Schulz B., Altieri B. et al., 1999, In: Terzian Y., Khachikian E., Weedman D. (eds.), *Activity in galaxies and related phenomena*, Vol. 194, p. 145, IAU Symposium
- Crovisier J., Leech K., Bockelee-Morvan D., et al., 1997, *Sci* 275, 1904
- Crowther P.A., Beck S.C., Willis A.J., et al., 1999, *MNRAS* 304, 654
- Désert F.X., Boulanger F., Puget J.L., 1990, *A&A* 237, 215
- Dudley C.C., 1999, *MNRAS* 307, 553
- Gabriel C., 1998, PHT interactive analysis user manual PIA V7.3, ESA/VILSPA-SAI, <http://www.iso.vilspa.esa.es/manuals/>
- Genzel R., Lutz D., Sturm E., et al., 1998, *ApJ* 498, 579
- Guillois O., Ledoux G., Nenner I., Papoular R., Reynaud C., 1998, In: d'Hendecourt L., Joblin C., Jones A. (eds.), *Solid interstellar matter: the ISO revolution*, Vol. 11, p. 103, Les Houches Workshop
- Hanner M.S., Lynch D.K., Russell R.W., 1994, *ApJ* 425, 274
- Heisler C.A., Vader J.P., 1994, *AJ* 107, 35
- Heisler C.A., Vader J.P., 1995, *AJ* 110, 87
- Heisler C.A., De Robertis M.M., Nadeau D., 1996, *MNRAS* 280, 579
- Heisler C.A., Lumsden S.L., Bailey J.A., 1997, *Nat* 385, 700
- Heisler C.A., Norris R.P., Jauncey D.L., Reynolds J.E., King E.A., 1998, *MNRAS* 300, 1111
- Kessler M.F., Steinz J.A., Anderegg M.E. et al., 1996, *A&A* 315, L27
- Langhoff S.R., 1996, *J. Phys. Chem. A* 100, 2819
- Laureijs R.J., 1998, In: d'Hendecourt L., Joblin C., Jones A. (eds.), *Solid interstellar matter: the ISO revolution*, Vol. 11, p. 33, Les Houches Workshop
- Laureijs R.J., Klaas U., Richards P.J., Schulz B., 1998, ISOPHOT data users manual, ESA, <http://www.iso.vilspa.esa.es/manuals/>, 4.0 edition
- Laurent O., Mirabel I.F., Charmandaris V., et al., 1999, In: Cox P., Kessler M.F. (eds.), *The universe as seen by ISO*, Vol. 2, p. 913, ESA
- Lemke D., Klaas U., Abolins J., et al., 1996, *A&A* 315, L64
- Lu N.Y., Helou G., Silbermann N. et al., 1999, In: Cox P., Kessler M.F. (eds.), *The universe as seen by ISO*, Vol. 2, p. 929, ESA
- Lutz D., Spoon H.W.W., Rigopoulou D., Moorwood A.F.M., Genzel R., 1998, *ApJ* 505, L103
- Malfait K., Waelkens C., Waters L.B.F.M., Vandenbussche B., Huygen E., de Graauw M.S., 1998, *A&A* 332, L25
- Metcalfe L., Steel S.J., Barr P., et al., 1996, *A&A* 315, L105
- Molster F.J., Yamamura I., Waters L.B.F.M., et al., 1999, *Nat* 401, 563
- Moorwood A.F.M., 1999, In: Cox P., Kessler M.F. (eds.), *The universe as seen by ISO*, Vol. 2, p. 825, ESA
- Moutou C., Sellgren K., Léger A., Verstraete L., Le Coupanac P., 1998, In: d'Hendecourt L., Joblin C., Jones A. (eds.), *Solid interstellar matter: the ISO revolution*, Vol. 11, p. 89, Les Houches Workshop
- O'Halloran B., Metcalfe L., Delaney M., et al., 1999, *A&A*, submitted
- Papoular R., Conrad J., Giuliano M., Kister J., Mille G., 1989, *A&A* 217, 204
- Peeters E., Tielens A.G.G.M., Roelfsema P.R., Cox P., 1999, In: Cox P., Kessler M.F. (eds.), *The universe as seen by ISO*, Vol. 2, p. 825, ESA
- Rigopoulou D., Genzel R., Lutz D., et al., 1999, In: Cox P., Kessler M.F. (eds.), *The universe as seen by ISO*, Vol. 2, p. 825, ESA
- Roche P.F., 1989, In: *Proc. 22nd Eslab symposium on infrared spectroscopy in astronomy*, p. 447, ESA SP-290
- Roelfsema P.R., Cox P., Tielens A.G.G.M., et al., 1996, *A&A* 315, L289
- Salama F., 1998, In: d'Hendecourt L., Joblin C., Jones A. (eds.), *Solid interstellar matter: the ISO revolution*, Vol. 11, p. 65, Les Houches Workshop
- Schaerer D., Contini T., Pindao M., 1999, *A&AS* 136, 35
- Schulz B., 1999, Long-term responsivity stability of ISOPHOT-S, Technical report, ESA
- Tielens A.G.G.M., Hony S., van Kerckhoven C., Peeters E., 1999, In: Cox P., Kessler M.F. (eds.), *The universe as seen by ISO*, Vol. 2, p. 825, ESA
- Uchida K.I., Sellgren K., Werner M., 1998, *ApJ* 493, L109
- Urry C.M., Padovani P., 1995, *PASP* 107, 803
- Vader J., Frogel J.A., Terndrup D.M., Heisler C.A., 1993, *AJ* 106, 1743
- Veilleux S., Osterbrock D.E., 1987, *ApJS* 63, 295
- Waelkens C., Malfait K., Waters L.B.F.M., 1998, *Ap&SS* 255, 25
- Waters L.B.F.M., Molster F.J., Waelkens C., 1998, In: d'Hendecourt L., Joblin C., Jones A. (eds.), *Solid interstellar matter: the ISO revolution*, Vol. 11, p. 219, Les Houches Workshop
- Watson D., Metcalfe L., Laureijs R.J., et al., 1999, in preparation
- Wills B.J., Wills D., Evans N.J.I., et al., 1992, *ApJ* 400, 96
- Young S., Hough J.H., Efstathiou A., et al., 1996, *MNRAS* 281, 1206